MARSNEXT MULTIPLE LANDER TARGETING TRAJECTORY COMPUTATION AND NAVIGATION

Daniel García Yárnoz [(1)], José Manuel Sánchez Pérez [(2)]

[(1)] GMV @ ESA/ESOC , Robert-Bosch-Str. 5, Darmstadt, Germany, Email:Daniel.Garcia@esa.int
[(2)]ESA/ESOC OPS-GFA, Robert-Bosch-Str. 5, Darmstadt, Germany, Email: Jose.Manuel.Sanchez.Perez@esa.int

ABSTRACT

The MarsNEXT mission is a technology demonstrator precursor to a future Mars Sample Return mission in the context of the Aurora program. One of its objectives is the delivery of a number of small landers to specific locations on the surface of Mars.

This paper provides a brief description of the algorithms implemented for the generation of trajectories consecutively deploying multiple landers, and finally inserting an orbiter around Mars. It also summarizes the results of a targeting and navigation analysis of three landers up to the Entry Interface Point (EIP) in Mars atmosphere. Two particularly attractive deployment sequences, representative of MarsNEXT mission design, are presented and analysed in more detail.

1. LANDER TARGETING PROBLEM

In the frame of the MarsNEXT mission analysis, the targeting problem of a planetary lander can be formulated as follows: given an initial state vector compute the manoeuvre that allows reaching the atmosphere entry point satisfying a given set of conditions. Generally, the time at which the manoeuvre must take place is defined by the operational schedule and is therefore considered an input parameter to the problem. Furthermore, optimality of the manoeuvre in terms of required ΔV is a desired feature of the searched trajectory.

The targeting problem can be formulated as a two-point boundary value problem with free final time. The state vector before the manoeuvre can be obtained just by numerical propagation from the initial state vector. Therefore, without loss of generality, the first point can be considered at the time of the manoeuvre from which only the position vector is known and the velocity vector must be solved in order to obtain the ΔV vector.
The end point is considered at entry into the atmosphere and its position is given relative to the planet. Thus the entry point is fixed to the planet equatorial rotating frame. The three components of the entry position vector are determined by the desired altitude, longitude and latitude.

Generally speaking, the positions of the initial and end points define the boundary value problem. In the case that the final time was fixed, this would lead to the well-known Lambert problem. However, for the targeting problem the entry time is in general free, leading to an optimization problem to obtain the desired trajectory. This optimization problem would have only one degree of freedom, namely the entry time.

If an additional condition is imposed to the targeting problem, the additional degree of freedom is removed in the optimization process. For entry trajectories, the Entry Descent and Landing (EDL) phase usually prescribes the entry angle that is required for safe landing. It seems meaningful then to impose the entry angle as a constraint. With fixed entry angle there are generally two solutions leading to the same entry point on the planet surface: one solution prograde, the other retrograde.

The final approach taken for the targeting algorithm has been a backwards formulation of the boundary value problem. Even if this problem requires no real optimization, it is formulated as the solution of a constrained optimization problem with:

- 3 variables: entry time, velocity modulus and the azimuth of the velocity vector.
- 3 constraints: difference of the position vector before and after the manoeuvre must be zero.

From the values of entry time, velocity modulus and azimuth the entry state vector is known and can be propagated backwards up to the manoeuvre time. There the difference of the position and velocity vectors is computed with respect to the given state vector previous to the manoeuvre. The difference of the position vector is the constraint to be made zero by the optimizer, while the difference of the velocity vector gives the manoeuvre ΔV.

Because the formulation of the problem automatically satisfies the conditions required at the entry point: position relative to the planet and entry angle, this approach has proved very successful to solve the targeting problem even with rough initial guesses for

the entry time, velocity modulus and azimuth. Some care must be taken to provide an initial guess for the azimuth leading to the required prograde or retrograde trajectory.

1.1 Release/Separation

One of the advantages of the backwards formulation described above is the simplicity to deal with the computation of the effect of the separation of the lander module.

Generally, separations of lander and carrier modules are provided by spring mechanisms. Ideally, the spring mechanism imparts a relative ΔV to the two parts along the separation longitudinal axis. The actual post-separation trajectories are obtained applying the conservation of the linear momentum law considering the masses of lander and carrier.

To ascertain a stable attitude at entry, the lander module symmetry axis must be aligned with the relative velocity at the atmospheric entry. Assuming that the attitude of the spinning lander module is kept constant during the ballistic arc from separation to entry, a constraint is imposed to the attitude at the separation. Namely, the ΔV imparted by the separation mechanism and the entry relative velocity must be aligned.

If the lander trajectory is computed backwards from the entry point to the separation, the direction of the separation ΔV is known, so that the fulfilment of the last condition can easily be introduced into the targeting problem without the need to add an additional constraint into the optimization. From the post-separation trajectory of the lander it is straightforward to compute the post-separation trajectory of the carrier and the pre-separation trajectory of the carrier+lander composite.

1.2 Errors at the Entry Interface Point

The covariance analysis method provides the evolution of the statistics of the errors associated to the determination of the state vector (knowledge) and the deviation of the actual state w.r.t. the reference state (dispersion). In this analysis the time is the independent variable and the knowledge/dispersion matrices can be propagated from an initial time to the final time using the SRIF method.

Some considerations must be regarded about the kind of errors applicable to the EDL analysis. The first one is the difference between errors at a fixed time coinciding exactly with the nominal entry time and the errors at fixed altitude. It should be noted that for this analysis a spherical planet and atmosphere have been assumed in the definition of the fixed altitude constraint.

The errors at the nominal entry time can be provided directly via the covariance analysis just propagating the dispersion matrix up to the entry. At this time some of the states will be below the atmosphere interface altitude and some of them will be above leading to a dispersion in altitude. The flight path angle will also present a dispersion “at fixed time”.

However, what shall be regarded for the EDL analysis is the flight path angle dispersion when the spacecraft (S/C) is exactly at the atmosphere interface altitude. This error will be referred in this document as “at fixed altitude”. Both errors, at fixed time and at fixed altitude, are intrinsically different in nature.

In order to obtain the errors at fixed altitude, a transformation must be applied to the dispersion matrix. This transformation is obtained from the linearised dynamics and has to be applied such as to cancel the altitude errors. By calculating the derivative of the radius w.r.t. the time we obtain Eq. 1, where V is the modulus of the velocity and γ is the flight path angle (FPA) particularized at the nominal entry point. For entry trajectories only negative flight path angles are regarded such that radius and altitude decrease with time.

$$\frac{dr}{dt} = V \sin\gamma \tag{1}$$

Deviations of the radius can be compensated by time deviations with opposite sign (Eq. 2)

$$\delta t = -\frac{\delta r}{V \sin\gamma} \tag{2}$$

In this way, state vectors above the atmosphere interface altitude are compensated by propagating a positive amount of time until reaching the desired altitude. State vectors below are propagated a negative amount of time (backwards propagation). This simple idea applied to the state vector linearised dynamics leads to a 6x6 transformation matrix. The dispersion matrix is transformed to fixed altitude by pre-multiplication and transpose post-multiplication with the transformation matrix.

A second issue regarding the errors at the entry point appears because of the difference between the inertial velocity vector and the relative velocity w.r.t. the rotating planet. Integration of the trajectory is performed in an inertial frame, so that the dispersion matrix at the entry point obtained via the covariance method usually is expressed in terms of the inertial velocity vector. However, entry trajectories in an atmosphere are subject to aerodynamic forces that depend on the relative velocity vector. Therefore, of interest for the EDL phase is the input of the errors related to the relative velocity vector.

The relation between inertial and relative velocity vectors is a linear transformation depending only on the components of the planet angular velocity vector and the state vector. Thus this linear transformation expressed in matrix form can be applied to the dispersion matrix to perform the change from inertial to relative velocity vector. This leads to basic algebraic manipulation of the dispersion matrix.

2. TRAJECTORY CALCULATION

2.1 Interplanetary Transfer

A detailed description of the different options for the transfer to Mars can be found in the Mission Analysis Guidelines for MarsNEXT [1]. For this lander deployment and subsequent navigation analysis, the 2017T4 transfer was selected. Fig. 1 and Fig. 2 show the geometry of the 2017T4 interplanetary transfer. The hyperbolic arrival velocity at Mars and approximate arrival time obtained from this trajectory are inputs for the lander deployment sequence definition.

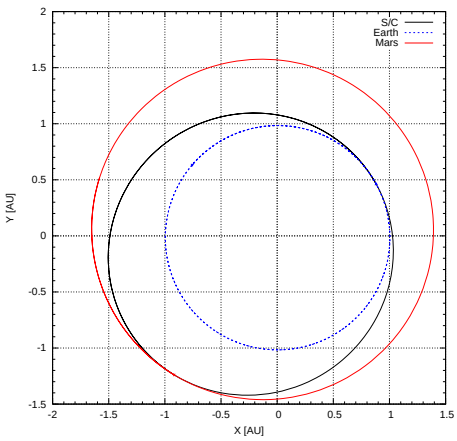

Fig. 1. Interplanetary transfer trajectory XY-projection in Ecliptic 2000 frame

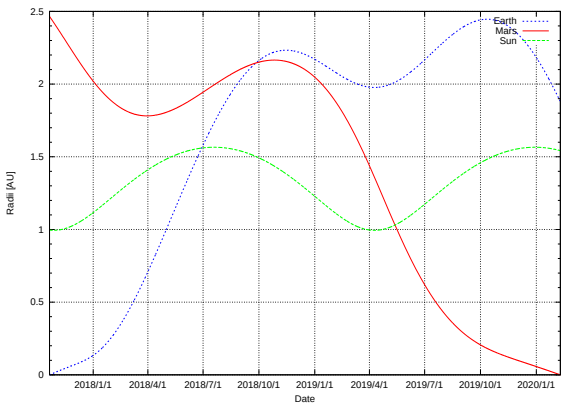

Fig. 2. Distances to Earth, Mars and Sun

Previous studies performed as part of the MARSNET phase A feasibility studies [2], [3] can serve as background for this analysis.

2.2 Lander Retargeting Costs

For the delivery of several landers from hyperbolic trajectory at different locations on the surface of Mars, retargeting manoeuvres are required. The range of longitudes and latitudes that the entry points should cover is still under definition. In order to estimate the costs of retargeting to a different EIP latitude and longitude, a parametric analysis was performed.

For this analysis, the targeting and deployment of landers from the previously calculated hyperbolic arrival is considered. The constraints are imposed on the EIP instead of the landing point, which would require a more detailed analysis of the atmospheric flight. The EIP altitude, assuming spherical planet and atmosphere, is set to 120 km.

An initial hyperbolic arrival with a target EIP of 0° in longitude and latitude and a target FPA with respect to a rotating frame of -14° is considered. The longitude of the entry point is an arbitrary reference longitude in the equatorial Mars rotating reference frame. It can be shifted to any reference longitude by modifying the arrival date. From this arrival trajectory, a retargeting manoeuvre is performed 7 days before entry, to a second EIP with the same target FPA and different longitude and latitude. The initial and final hyperbolic approach can be either prograde or retrograde.

Fig. 3 plots the retargeting ΔV costs in a longitude-latitude grid for two different cases: retargeting from a prograde transfer to a prograde one, and from prograde to retrograde. The x-axis represents a relative longitude change with respect to the reference one. The plots for the missing cases retrograde to retrograde, and retrograde to prograde are almost symmetric w.r.t. zero longitude change.

The results show that the retargeting costs are mostly dependant on the desired variation in longitude, while a change in the target latitude requires relatively low ΔV. If the orientation (prograde vs. retrograde) of the approach hyperbola is not changed, the optimal variation in longitude is near zero. A change in the orientation allows for a cheap change in longitude of around 150° east for a prograde-to-retrograde retargeting, and symmetrically 150° west for a retrograde-to-prograde one. The non-symmetry with respect to the equator of the plots is due to the fact that the incoming hyperbolic velocity has a non-zero declination with respect to Mars equator (for our trajectory the declination is around -9°). If the initial target latitude is different from zero, similar plots can be obtained

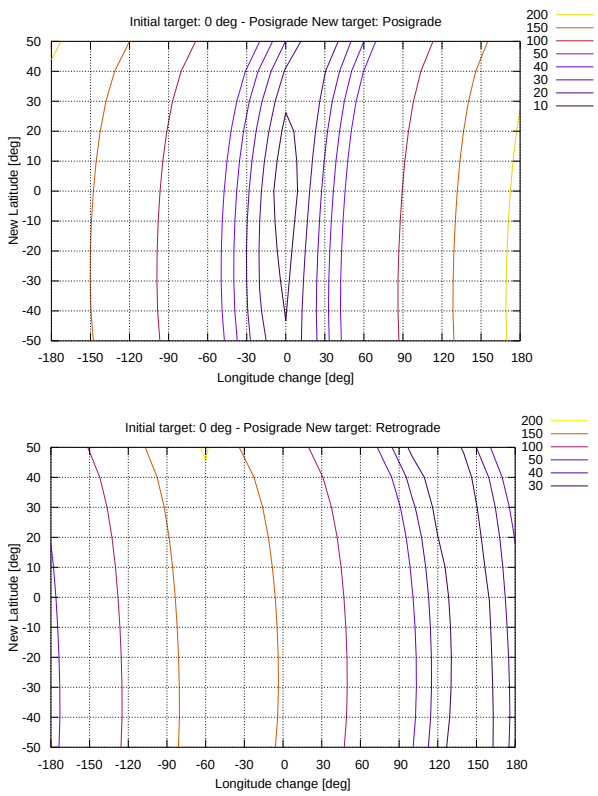

Fig. 3. Retargeting ΔV costs from an initial prograde target. The new entry trajectory is prograde (above) or retrograde (below)

3.3 Single Lander Entry FPA Errors

An interesting first result that can be obtained with covariance analysis is the FPA errors for a single lander considering only separation errors in the release mechanism. It allows determining an upper limit for the release time prior to entry.

A parametric analysis has been performed to study the dispersion in FPA at entry as a function of the release date. For this analysis, the nominal residual ΔV at separation is set to 0.5 m/s. A 5% 3-σ error in the ΔV modulus and a 4° 3-σ error in direction are assumed. All other navigation errors or sources of dispersion previous to the separation are considered negligible. The target FPA in a rotating frame has been again set to -14°. The target reference longitude is arbitrarily fixed to 0°, while three different target latitudes (30°, 0° and -30°) are included to study its effect.

The obtained FPA dispersion at fixed time increases linearly with the separation time, it is similar for both prograde and retrograde entries and it is not much affected by the target latitude. When considering the inertial FPA at fixed altitude the error is greater for prograde entries. A shallower inertial entry angle (-13.4°) is required for prograde transfers than for retrograde ones (which present a steeper -14.6°), in order to obtain the same relative entry angle in a rotating frame of -14°, the ultimate reason being the rotation of the planet. This shallower inertial entry angle translates into a higher dispersion when transforming the errors from fixed time to fixed altitude for the prograde transfers.

When changing to FPA dispersion in a rotation frame (see Fig. 4), the difference between prograde and retrograde transfers is more evident. Error in prograde transfers increases slightly, while in retrograde it decreases, but the general trend is the same.

A first conclusion can be drawn from this analysis. If the dispersion of the entry angle in a rotating frame is limited to 1° 3-σ, then the earliest release of the first lander for a prograde transfer would be 14 days with the current assumptions, assuming that all other sources of errors have been eliminated. This tightens the deployment schedule if 3 landers are supposed to be released. In the case of a retrograde transfer the first lander earliest release date could be increased up to 17 days before entry.

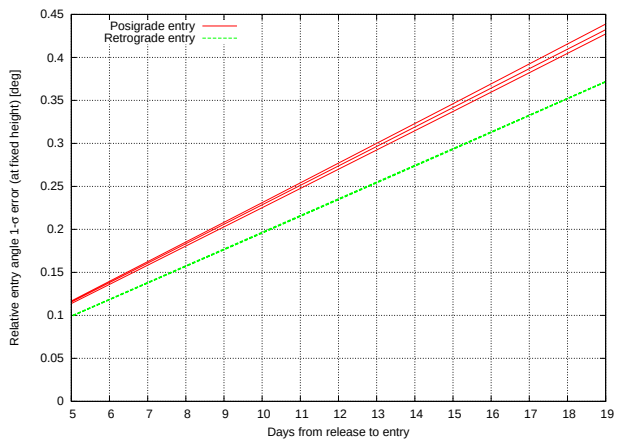

Fig. 4. Rotating frame entry angle errors at fixed entry altitude of a single lander as a function of the release time. Three different target latitudes (30, 0 and -30°) are shown for a prograde and a retrograde entry.

Possible mitigation measures are the reduction of the size of the ΔV at separation or its deviation from nominal execution.

The FPA dispersion at entry is a relevant parameter for the mission design. Assuming a fixed FPA dispersion of ±1° 3-σ at the EIP, Fig. 5 provides the earliest release time for a prograde entry as a function of the ΔV error in modulus and direction introduced by the separation mechanism. It does not take into consideration any other sources of dispersion in the trajectory. If early releases of the first lander are desired, a requirement in the size of the ΔV at separation (either in the magnitude of the manoeuvre or in the level of error) is necessary.

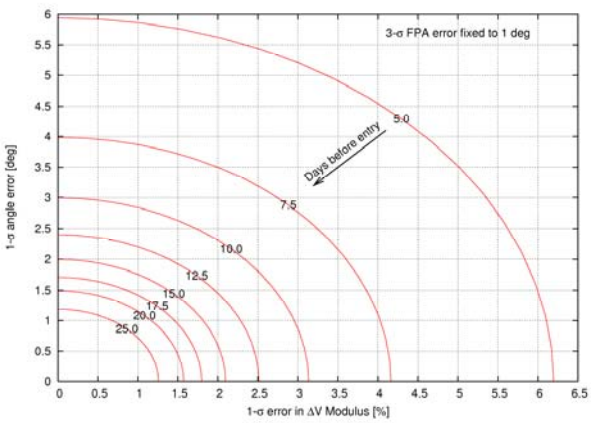

Fig. 5. Earliest release time for prograde entry as a function of separation mechanism errors (modulus and direction) . The FPA error is fixed at ±1° 3-σ. The separation ΔV of is 0.5 m/s.

3.3 Lander Deployment Sequence

Two full lander deployment sequences have been designed using the previously described methodology. They comprise the targeting and deployment of three landers (L1, L2 and L3) from a hyperbolic approach trajectory up to the EIP at 120 km altitude. The initial mass of the composite (carrier plus three landers) is assumed to be 1500 kg, with each of the landers weighting 125 kg. The initial approach trajectory is already targeting the EIP of the first lander. This has been set to -8° longitude and -2° latitude (landing site close to crater Miyamoto). The target flight path angle at entry for all three landers is -14°. The separation mechanism ΔV is assumed 0.5 m/s.

Two tentative initial sequences were designed taking into account the retargeting costs and the minimum delivery errors presented. The first lander is released 13 days before EIP, close to the earliest release date, to minimize the subsequent retargeting ΔVs and allow for small enough dispersion in FPA at entry. The other two lander separations are spaced 4 days apart form each other (days -9 and -5 w.r.t. EIP date), and the retargeting manoeuvres take place one day before each separation. The first retargeting manoeuvre for L1 is null, as the S/C is already in the correct trajectory. One day after the third lander separation, an additional reorbiting manoeuvre takes place to target the conditions for Mars Orbit Insertion (MOI) at an orbit of 500 km periares height and 45° inclination. When giving relative dates the EIP of the first lander is used as reference. These sequences are later discussed and redesigned to improve the overall performance of the lander targeting and navigation.

The third body perturbation of the Sun is considered in the propagation of all phases.

RPP SEQUENCE:

The first sequence presented has an initial retrograde hyperbolic approach targeting the first lander EIP conditions. The second and third landers follow prograde approach trajectories with target longitudes of -160 and -150° respectively. This results in low retargeting ΔV (as it was shown in section 2.2). The target latitudes are chosen arbitrarily -30 and 30° respectively, to cover a wider range of latitudes. Four days before EIP a final reorbiting manoeuvre of 4 m/s retargets the carrier to its insertion orbit conditions. The total ΔV costs for the retargeting of landers 2 and 3 and the carrier is 36.09 m/s. Table 1 presents the event sequence for this RPP trajectory.

Table 1. Tentative lander deployment sequence for test case RPP, three landers with retrograde-prograde-prograde entries. The first column provides number of days relative to the EIP of the first separated lander.

Day	Event				
-20	START	V_{inf}	[km/s]	2.530	
		2-D Impact Vect.	[km]	-6938.2	74.4
-13	SEP L1	ΔV L1 | Carrier	[m/s]	0.458	0.042
-10	ΔV2	ΔV	[m/s]	16.653	
		2-D Impact Vect.	[km]	6761.6	-3795.7
-9	SEP L2	ΔV L2 | Carrier	[m/s]	0.455	0.045
-6	ΔV3	ΔV	[m/s]	15.794	
		2-D Impact Vect.	[km]	6153.1	4461.9
-5	SEP L3	ΔV L3 | Carrier	[m/s]	0.450	0.050
-4	REORB	ΔV	[m/s]	3.641	
0	EIP L1	Longit. | Latit.	[deg]	-8.00	-2.00
		FPA Inert. | Rotat.	[deg]	-14.62	-14.00
		Solar Hour	[h]	23.13	
		2-D Impact Vect.	[km]	-7459.0	116.8
0.02	EIP L2	Longit. | Latit.	deg]	-160.00	-30.00
		FPA Inert. | Rotat.	[deg]	-13.46	-14.00
		Solar Hour	[h]	13.40	
		2-D Impact Vect.	[km]	6593.8	-3591.0
0.03	EIP L3	Longit. | Latit.	deg]	-150.00	30.00
		FPA Inert. | Rotat.	[deg]	-13.51	-14.00
		Solar Hour	[h]	14.19	
		2-D Impact Vect.	[km]	6044.0	4462.1
0.03	PERIC.	Height	[km]	500.0	
		Inclination	[deg]	45.0	

PPP SEQUENCE:

The second sequence considered has a prograde hyperbolic approach for all three landers. This has the benefit of daylight landings for the three landers, while in the previous case the first landing was at the night side of the planet (notice the solar hour in Tables 1 and 2). The second and third landers have target longitudes of 110 and 100° respectively, and the target longitudes are 30 and -30. The retargeting ΔV for the second lander is thus greater than in the RPP case (84 m/s). The total ΔV costs for the retargeting of landers 2 and 3 and the carrier is 106.98 m/s. The higher cost is due to the large retargeting manoeuvre for L2. Table 2 presents the event sequence for this PPP trajectory.

Note that in this sequence the first released lander enters the atmosphere last.

Table 2. Tentative lander deployment sequence for test case PPP, three landers with prograde-prograde-prograde entries. The first column provides number of days relative to the EIP of the first separated lander.

Day	Event				
-20	START	V_{inf}	[km/s]	2.530	
		2-D Impact Vect.	[km]	7093.2	431.5
-13	SEP L1	ΔV L1 | Carrier	[m/s]	0.458	0.042
-10	ΔV2	ΔV	[m/s]	83.986	
		2-D Impact Vect.	[km]	6163.0	4493.3
-9	SEP L2	ΔV L2 | Carrier	[m/s]	0.455	0.045
-6	ΔV3	ΔV	[m/s]	16.147	
		2-D Impact Vect.	[km]	6550.7	-3478.2
-5	SEP L3	ΔV L3 | Carrier	[m/s]	0.450	0.050
-4	REORB	ΔV	[m/s]	6.846	
-.32	EIP L3	Longit. | Latit.	[deg]	100.00	-30.00
		FPA Inert. | Rotat.	[deg]	-13.46	-14.00
		Solar Hour	[h]	13.34	
		2-D Impact Vect.	[km]	6414.7	-3488.2
-.31	PERIC.	Height	[km]	500.0	
		Inclination	[deg]	45.0	
-.31	EIP L2	Longit. | Latit.	deg]	110.00	30.00
		FPA Inert. | Rotat.	[deg]	-13.51	-14.00
		Solar Hour	[h]	14.13	
		2-D Impact Vect.	[km]	5906.4	4301.1
0	EIP L1	Longit. | Latit.	deg]	-8.00	-2.00
		FPA Inert. | Rotat.	[deg]	-13.39	-14.00
		Solar Hour	[h]	13.57	
		2-D Impact Vect.	[km]	7498.2	160.7

3. NAVIGATION ANALYSIS

A navigation analysis was performed for the lander deployment sequences presented. A batch sequential SRIF filter and a fixed time guidance law as implemented in INTNAV [4], together with further extensions for deterministic manoeuvre errors described in [5], have been used to perform the covariance and guidance analysis.

4.1 Assumptions and Models

The following measurements have been considered in the analysis:

- Range from Cebreros and New Norcia. Minimum elevation 10°.
- Doppler from Cebreros and New Norcia. Minimum elevation 10°.
- ΔDOR from two possible baselines Cebreros-New Norcia (C-N) and Santiago-Cebreros (S-C). Minimum elevation 15°. One measurement every 4 days, one measurement per day in critical phases.

The following errors can be accounted for in the analysis:

- Initial S/C position: 100 km 1-σ dispersion and 1000 km 1-σ knowledge
- Initial S/C velocity: 1 m/s 1-σ dispersion and 10 m/s 1-σ knowledge
- Range: 20 m 1-σ random noise and 2 m 1-σ bias
- Doppler: 0.3 mm/s 1-σ random noise
- ΔDOR: 6 cm 1-σ random noise.
- Non-gravitational acceleration: exponentially correlated random variable with $6 \cdot 10^{-12}$ km/s^2 1-σ noise and a correlation time of 1 day
- Lander separation ΔV errors: 1.667% 1-σ in modulus and 1.333° 1-σ in direction (conical error)
- Deterministic and trajectory correction manoeuvres (TCM) ΔV errors: 0.6% 1-σ in modulus and 0.5° 1-σ in direction (conical error)

All errors are conservative. No solar radiation pressure has been taken into account.

4.2 Navigation results

The navigation analysis performed starts 50 days before arrival with the initial knowledge and dispersion assumptions indicated. The initial knowledge assumption is particularly pessimistic; however, after processing the first batch of measurements knowledge levels drop independently of the initial values selected. Two TCM slots (10 days after start and one day before separation of L1) are available before the separation of L1, to eliminate the effect of the initial arbitrary dispersion considered. This provides a realistic dispersion ellipsoid without having to deal with the whole interplanetary trajectory. These ΔVs should not be budgeted. Instead, results from the interplanetary navigation analysis for the approach navigation should be used. The main sources of dispersion in the trajectory are the errors in the execution of the deterministic ΔVs. After lander separation, there are no further corrections or other type of guidance assumed.

Range and Doppler from two stations is always considered for all the analysis performed. ΔDOR can be considered from one or two baselines (Cebreros-New Norcia and Santiago-Cebreros, the stations of the other possible baseline do not have visibility of the S/C simultaneously). ΔDOR measurement frequency can be increased to one measurement per day after the retargeting manoeuvres ΔV2 and ΔV3 until the TCM slot before separation.

In the described sequences, retargeting manoeuvres for the conditions of lander 2 entry, lander 3 entry and carrier insertion take place 10, 6 and 4 days before arrival. Separations of L2 and L3 occur only one day after the first two retargeting manoeuvres. A trajectory correction manoeuvre is required between retargeting and separation of the landers (or final insertion of the

carrier) to correct the dispersion introduced by the execution errors of the retargeting manoeuvre. There is short time available for orbit determination, even if the 3TCM slot is delayed until immediately before separation. This presents also operational problems.

If the retargeting manoeuvres are advanced to day -12 and -8 (1 day after separation of L1 and L2), the cleanup TCMs can also be advanced to one day before separation of L2 and L3. This has two immediate benefits: the size of the retargeting manoeuvres ΔV2 and ΔV3 is reduced, and there are two days for orbit determination before the TCMs. The total deterministic ΔV is reduced to 30 m/s and 88 m/s for cases RPP and PPP respectively. The least favoured lander is still L2, because its separation takes place after the larger ΔV (especially in PPP sequences). There is the possibility to increase the ΔDOR frequency to daily measurements after these manoeuvres in order to improve the lander delivery.

Fig. 6 shows a schematic representation of the two scenarios described above. The timelines show the TCM slots (downward arrows), as well as the retargeting manoeuvres and separations of landers.

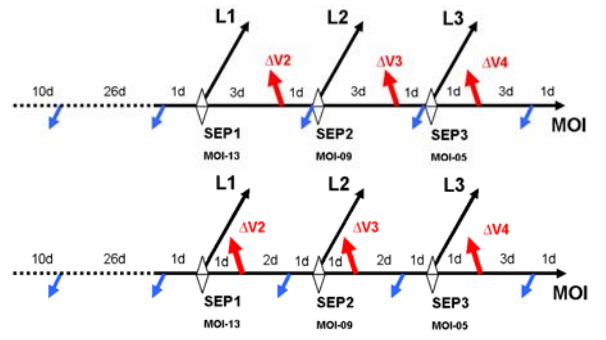

Fig. 6. Schematic representations of the navigation strategies. TCM slots are represented with blue arrows

Table 3 presents the results of the navigation analysis for RPP and PPP sequences for different measurement strategies and the two timelines described. For the second timeline, the effect of the inclusion of daily ΔDOR measurements is also analysed. The table contains the FPA errors at fixed altitude in Mars equatorial rotating frame for the three landers, as well as the final delivery errors at pericentre for the carrier. The errors of the carrier are given in semi-major and semi-minor axis of the dispersion ellipse at the periares plane, and the linearised time of flight at periares. The PPP sequence has, as expected, worse performance in terms of navigation than the RPP case. This is caused by the larger size of the ΔVs and the more unfavourable achievable errors in FPA at fixed altitude in a rotating frame. If errors in the FPA of ±1° 3-σ are required, the condition is not met for lander 2 in any of the cases studied.

Table 3. Navigation results for the initial PPP and RPP sequences.

Measurem. Strategy	Relative FPA 1-σ errors at fixed altitude [deg]			Carrier 1-σ Delivery Errors		
	L1	L2	L3	SMA [km]	smi [km]	LTF [s]
PPP CASE: 1 day orbit determination before TCM 2 and 3						
R & D only	0.461	6.110	3.093	23.497	0.916	7.465
ΔDOR C-N	0.311	4.365	1.025	17.026	0.853	5.483
ΔDOR S-C	0.356	3.222	0.949	12.990	0.826	4.506
ΔDOR 2 bas	0.309	3.159	0.934	12.563	0.783	4.472
PPP CASE: 2 days orbit determination before TCM 2 and 3						
R & D only	0.470	5.333	2.821	21.887	0.869	6.958
ΔDOR C-N	0.312	4.411	1.125	14.318	0.826	4.597
ΔDOR S-C	0.359	3.503	1.032	10.625	0.809	3.822
ΔDOR 2 bas	0.310	3.452	1.015	10.479	0.771	3.800
ΔDOR C-N daily	0.312	0.941	0.570	13.886	0.824	4.449
ΔDOR S-C daily	0.359	0.569	0.467	10.274	0.809	3.722
ΔDOR 2 bas daily	0.310	0.544	0.359	10.055	0.769	3.656
RPP CASE: 1 day orbit determination before TCM 2 and 3						
R & D only	0.428	2.006	1.312	18.905	0.761	4.247
ΔDOR C-N	0.262	1.839	0.871	13.038	0.711	3.169
ΔDOR S-C	0.303	1.832	0.785	11.374	0.691	2.659
ΔDOR 2 bas	0.261	1.824	0.779	10.566	0.713	2.460
RPP CASE: 2 days orbit determination before TCM 2 and 3						
R & D only	0.432	1.948	1.218	17.857	0.730	4.110
ΔDOR C-N	0.263	1.624	0.759	11.109	0.686	2.893
ΔDOR S-C	0.305	1.805	0.809	8.451	0.685	2.185
ΔDOR 2 bas	0.262	1.586	0.731	8.179	0.712	2.116
ΔDOR C-N daily	0.263	0.889	0.557	10.733	0.682	2.837
ΔDOR S-C daily	0.305	0.470	0.272	6.862	0.683	1.959
ΔDOR 2 bas daily	0.262	0.408	0.257	6.742	0.708	1.913

4.2 Modified Lander Deployment Sequences

In order to improve the delivery accuracy of L2, modified lander deployment sequences were designed for the RPP and PPP case

In this modified sequences, lander 1 release is advanced by 2 days (worsening the minimum FPA error achievable for this lander). This allows advancing ΔV2 by the same number of days. The size of this manoeuvre is further reduced and now four days of orbit determination are available between ΔV2 and the TCM slot one day before separation of L2. Compared with the previous sequences, this sequence favours L2 delivery at the expense of the L1 delivery. The total

deterministic ΔV is reduced to 28 m/s and 78 m/s for cases RPP and PPP.

Tables 4 and 5 present a detailed timeline description of these sequences for RPP and PPP approach. Fig. 7 shows the new navigation strategy with additional time for orbit determination before L2 release.

Table 6 summarizes the results of the navigation analysis for the modified RPP and PPP sequences, for different measurement strategies, and the two timelines described. These sequences present an overall improvement for all cases in FPA errors at L2 EIP. However, the condition of ±1° 3-σ delivery accuracy for all three landers is only met in the RPP case when daily ΔDOR measurements from two baselines are assumed. In the PPP case with the same configurations, all three landers slightly exceed this limit.

Table 4. Modified lander deployment sequence for test case RPP, three landers with retrograde-prograde-prograde entries. The first column provides number of days relative to the EIP of the first separated lander.

Day	Event				
-20	START	V_{inf}	[km/s]	2.530	
		2-D Impact Vect.	[km]	-6858.2	68.3
-15	SEP L1	ΔV L1 | Carrier	[m/s]	0.458	0.042
-14	ΔV2	ΔV	[m/s]	11.861	
		2-D Impact Vect.	[km]	6759.1	-3795.7
-9	SEP L2	ΔV L2 | Carrier	[m/s]	0.455	0.045
-8	ΔV3	ΔV	[m/s]	11.914	
		2-D Impact Vect.	[km]	6148.2	4462.2
-5	SEP L3	ΔV L3 | Carrier	[m/s]	0.450	0.050
-4	REORB	ΔV	[m/s]	3.628	
0	EIP L1	Longit. | Latit.	[deg]	-8.00	-2.00
		FPA Inert. | Rotat.	[deg]	-14.62	-14.00
		Solar Hour	[h]	23.13	
		2-D Impact Vect.	[km]	-7459.0	116.8
0.02	EIP L2	Longit. | Latit.	deg]	-160.00	-30.00
		FPA Inert. | Rotat.	[deg]	-13.46	-14.00
		Solar Hour	[h]	13.41	
		2-D Impact Vect.	[km]	6590.8	-3590.7
0.03	EIP L3	Longit. | Latit.	deg]	-150.00	30.00
		FPA Inert. | Rotat.	[deg]	-13.51	-14.00
		Solar Hour	[h]	14.20	
		2-D Impact Vect.	[km]	6038.8	4462.0
0.03	PERIC.	Height	[km]	500.0	
		Inclination	[deg]	45.0	

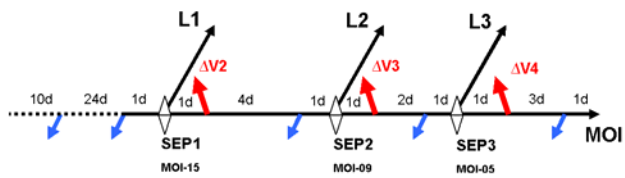

Fig. 7. Schematic representation of the navigation strategy for the modified sequence.

Table 5. Modified lander deployment sequence for test case PPP, three landers with retrograde-prograde-prograde entries. The first column provides number of days relative to the EIP of the first separated lander.

Day	Event				
-20	START	V_{inf}	[km/s]	2.530	
		2-D Impact Vect.	[km]	7031.5	472.3
-15	SEP L1	ΔV L1 | Carrier	[m/s]	0.458	0.042
-14	ΔV2	ΔV	[m/s]	59.013	
		2-D Impact Vect.	[km]	6196.9	4541.7
-9	SEP L2	ΔV L2 | Carrier	[m/s]	0.455	0.045
-8	ΔV3	ΔV	[m/s]	12.107	
		2-D Impact Vect.	[km]	6599.8	-3507.2
-5	SEP L3	ΔV L3 | Carrier	[m/s]	0.450	0.050
-4	REORB	ΔV	[m/s]	6.886	
-.32	EIP L3	Longit. | Latit.	[deg]	100.00	-30.00
		FPA Inert. | Rotat.	[deg]	-13.46	-14.00
		Solar Hour	[h]	13.36	
		2-D Impact Vect.	[km]	6464.1	-3516.9
-.31	PERIC.	Height	[km]	500.0	
		Inclination	[deg]	45.0	
-.31	EIP L2	Longit. | Latit.	deg]	110.00	30.00
		FPA Inert. | Rotat.	[deg]	-13.51	-14.00
		Solar Hour	[h]	14.16	
		2-D Impact Vect.	[km]	5940.8	4348.3
0	EIP L1	Longit. | Latit.	deg]	-8.00	-2.00
		FPA Inert. | Rotat.	[deg]	-13.39	-14.00
		Solar Hour	[h]	13.57	
		2-D Impact Vect.	[km]	7498.2	160.7

Table 6. Navigation results for the modified PPP and RPP sequences.

Measurem. Strategy	Relative FPA 1-σ errors at fixed altitude [deg]			Carrier 1-σ Delivery Errors		
	L1	L2	L3	SMA [km]	smi [km]	LTF [s]
PPP CASE						
R & D only	0.526	3.569	2.285	21.253	0.855	6.778
ΔDOR C-N	0.357	3.315	1.090	14.422	0.821	4.642
ΔDOR S-C	0.404	3.031	1.021	10.646	0.802	3.840
ΔDOR 2 bas	0.355	3.015	1.007	10.491	0.764	3.817
ΔDOR C-N daily	0.357	0.693	0.562	13.964	0.819	4.484
ΔDOR S-C daily	0.404	0.364	0.469	10.277	0.802	3.732
ΔDOR 2 bas daily	0.355	0.357	0.359	10.047	0.762	3.666
RPP CASE						
R & D only	0.483	1.810	1.133	17.573	0.728	4.065
ΔDOR C-N	0.301	1.618	0.755	11.203	0.688	2.915
ΔDOR S-C	0.342	1.717	0.779	8.529	0.685	2.199
ΔDOR 2 bas	0.301	0.548	0.554	10.835	0.683	2.861
ΔDOR C-N daily	0.342	0.370	0.271	6.869	0.683	1.961
ΔDOR S-C daily	0.300	1.591	0.721	8.234	0.712	2.125
ΔDOR 2 bas daily	0.300	0.284	0.256	6.746	0.708	1.914

Table 7 contains the summary of the trajectory correction manoeuvre effect for the modified RPP sequence. The 1-σ dispersion propagated until target point is given before and after the TCMs. The target points are the EIP of L1 (first two manoeuvres), L2 and L3, and the MOI periares. The total navigation ΔV allocation is less than 5.5 m/s. The main contributor is the first TCM, which is proportional to the initial arbitrary dispersion assumed for the navigation analysis. For the PPP case the size of TCM3 increases to 1.73 m/s, as it has to correct the dispersion introduced by the execution errors of the larger retargeting manoeuvre. The total allocation stays below 7 m/s.

Fig. 8 plots for the RPP case the evolution of the position dispersion and knowledge mapped to the target point, in its along-track, cross-track and radial components. Each subplot represents one of the S/C: landers 1 to 3 and carrier. It is possible to identify the drops in dispersion down to the level of knowledge every TCM, and the sudden increase in dispersion after the deterministic retargeting manoeuvre, and, in a smaller scale, after the separation residual ΔVs.

Fig. 9 plots for the RPP case the evolution of the velocity knowledge in its along-track, cross-track and radial components. Each subplot represents one of the S/C: landers 1 to 3 and carrier. Every single manoeuvre (TCMs, deterministic and separation) deteriorates the velocity knowledge. The 4-day frequency of the ΔDOR measurements can be easily observed by the improvements in knowledge especially in the Lander 1 subplot. The daily measurements after ΔV2 and ΔV3 and its improvement in knowledge are observable in L2 and L3 subplots. This could be further improved by estimation of the manoeuvre execution errors.

Table 7. TCM summary for modified RPP sequence with ΔDOR measurements assumed from two baselines (daily frequency after ΔV2 and ΔV3).

	Time Target	ΔV 99% [m/s]		SMA [km]	Smi [km]	LTF [s]
TCM1	T0+10 EIP L1	4.255	Error-	3228.43	1898.51	1833.93
			Error+	34.01	21.63	20.61
TCM2	SEP1-1 EIP L1	0.119	Error-	34.59	21.98	20.95
			Error+	3.89	1.76	2.12
TCM3	SEP2-1 EIP L2	0.344	Error-	62.33	39.80	38.22
			Error+	5.40	2.15	4.24
TCM4	SEP3-1 EIP L3	0.327	Error-	36.83	22.81	22.23
			Error+	6.34	2.45	4.67
TCM5	MOI-1 MOI	0.353	Error-	8.36	3.86	4.84
			Error+	6.75	0.71	1.91

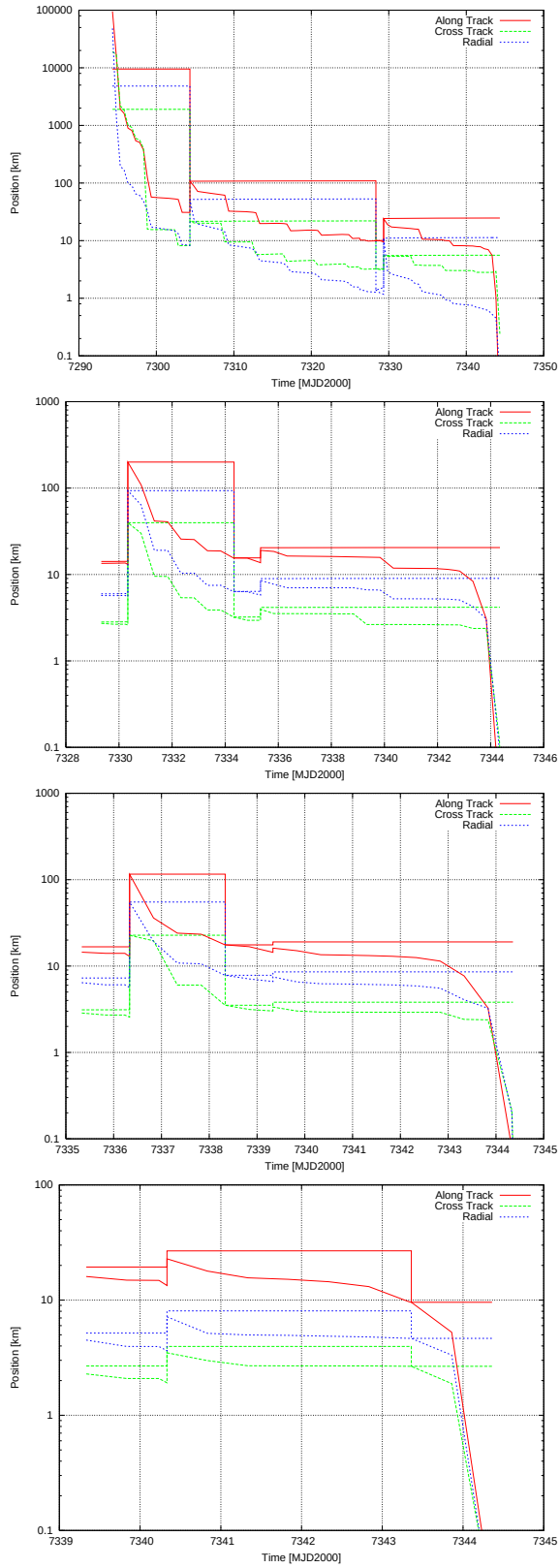

Fig. 8. Position knowledge and dispersion (1-σ) evolution for L1, L2, L3 and Carrier of RPP modified sequence. The knowledge and dispersion have been mapped to the target point (EIP or MOI).

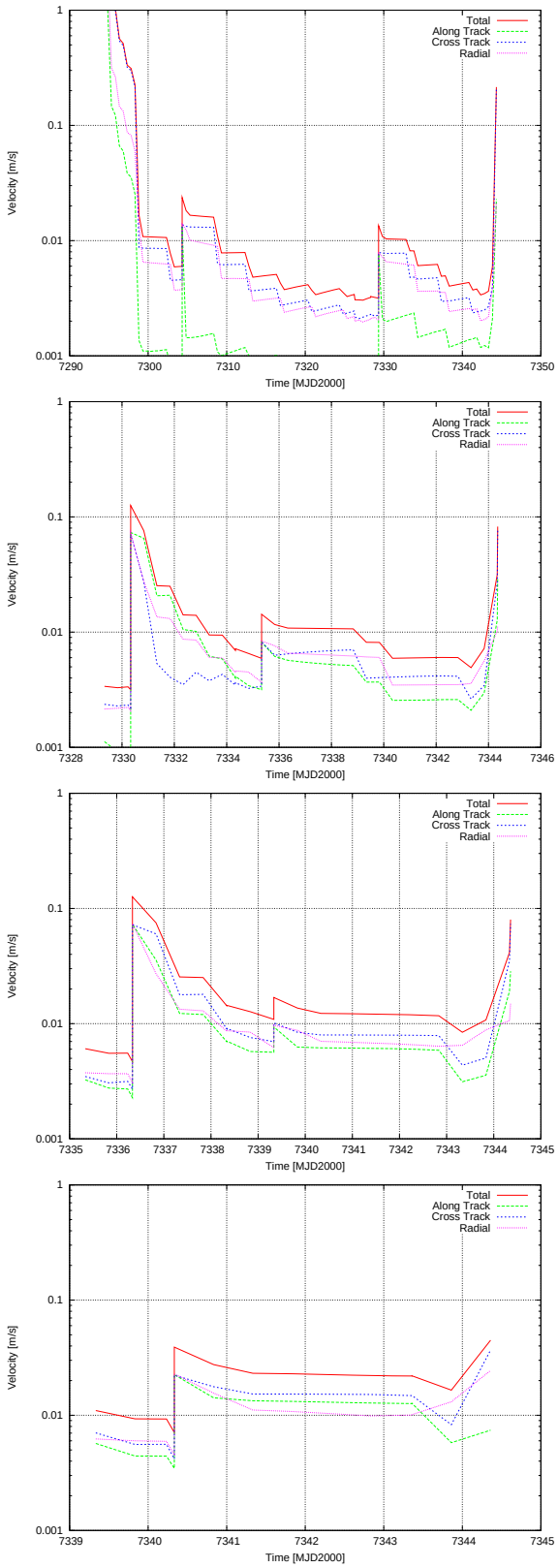

Fig. 9. Velocity knowledge and dispersion (1-σ) evolution for L1, L2, L3 and Carrier of RPP modified sequence.

4. CONCLUSIONS

The proposed backward formulation for lander targeting problems is an effective approach for the design of trajectories with multiple lander retargeting. It is well suited for the inclusion of lander release mechanism induced ΔV and any number of retargeting manoeuvres.

An analysis of the landing site targeting has been carried out for the MarsNEXT mission. Two attractive sequences comprising the retargeting and deployment of three landers at Mars have been presented and a detailed navigation analysis has been presented.

The results of the analysis show:

- Errors in the ΔV induced by the lander release mechanism establish a minimum error in FPA for a given separation date, as there is no control or corrections of the lander trajectory after separation. This limits the earliest day that the first lander can be released. Retrograde trajectories present smaller errors in FPA than prograde ones.
- Execution errors of the retargeting deterministic manoeuvres are the biggest contributors of errors in FPA at EIP. A TCM after each retargeting manoeuvre and before next lander separation is required to reduce FPA errors to acceptable levels.
- An effective measure to mitigate the effect of these errors and increase the accuracy of the TCMs is the planning of daily ΔDOR measurements after retargeting manoeuvres to quickly recover the knowledge before next TCMs. They allow reducing the delivery errors in FPA of all landers at EIP to less than 0.36° 1-σ in the case of a prograde-prograde-prograde sequence, and less than 0.3° 1-σ in the case of a retrograde-prograde-prograde sequence.

As a first outcome of the present analysis we strongly recommend to consider the inclusion of daily ΔDOR measurements from two baselines as a requirement during the approach, release of landers and insertion at Mars.

5. REFERENCES

1. Khan, M., *NEXT Mars Orbiter Mission: Mission Analysis Guidelines (MAS WP516),* NEXT-MO-MAG-ESA(HME)-0001, Is. 1 Rev. 1, 02 Nov. 2007.

2. Lauer M. & Hechler M., *Targeting of Several Mars Landers*, AIAA Journal of Guidance, Control, and Dynamics Vol. 17, No. 1, pp. 109-115, 1994.

3. Hechler M. & Lauer M., *Approach Navigation for Delivery of Small Landers to the Surface of Mars*,

AIAA Journal of Guidance, Control, and Dynamics Vol. 17, No. 1, pp. 116-122, 1994.

4. Belló, M. & Baeza, M., *Software Tool for Interplanetary Navigation Final Report*, GMV, ESA Contract No. 9715-91-D-IM, 1992.

5. Sánchez Pérez, J. M. &, Rodríguez Canabal, J. L., ROSETTA Mission Analysis: Interplanetary Trajectory Navigation, WP447, ESA-ESOC, 2002